JETIR.ORG ISSN: 2349-5162 | ESTD Year : 2014 | Monthly Issue
JOURNAL OF EMERGING TECHNOLOGIES AND INNOVATIVE RESEARCH (JETIR)
An International Scholarly Open Access, Peer-reviewed, Refereed Journal

ADSORPTION STUDIES OF BASIC VIOLET 14 AND DIRECT YELLOW 12 DYE REMOVALS FROM TEXTILE WASTEWATER USING WHEAT BRAN ADSORBENT

Pinki Rani[1], Dr. Heena Dahiya[2], Dr.Shikha Govil[3]

[1]Research Scholar, Baba Mastnath University, Rohtak, Haryana (India)

[2]Assistant Professor, Baba Mastnath University, Rohtak, Haryana (India)

[3]Associate Professor, G.L.bajaj Group of Institution, Mathura (India)

Email id of corresponding Author: pinkirani0311@gmail.com

Abstract: The present study investigates the potential of wheat bran as an effective biosorbent for the removal of Basic Violet 14 and Direct Yellow 12 dyes from aqueous solutions. The adsorbent was characterized using Fourier Transform Infrared Spectroscopy (FTIR), Scanning Electron Microscopy (SEM), X-ray Diffraction (XRD), and UV-Vis absorption spectroscopy to analyze its structural and surface properties. A series of batch adsorption experiments were conducted to evaluate the effects of key operational parameters, including initial dye concentration, contact time, solution pH, adsorbent dosage, and temperature, on adsorption efficiency. Kinetic modeling using pseudo-first-order and pseudo-second-order equations revealed that the adsorption process followed the pseudo-second-order model, suggesting chemisorption as the dominant mechanism. Equilibrium studies demonstrated that the adsorption behavior was well described by both Langmuir and Freundlich isotherms, indicating the coexistence of monolayer and multilayer adsorption. Thermodynamic analysis confirmed the spontaneous and endothermic nature of the adsorption process, with adsorption efficiency increasing at higher temperatures. The maximum adsorption capacities identified in this study highlight wheat bran's potential as a cost-effective, renewable, and efficient biosorbent for dye removal. These findings reinforce the viability of agricultural by-products as sustainable materials for wastewater treatment, offering an eco-friendly approach to mitigating industrial dye pollution.

Keywords: Adsorption, Basic Violet 14, Direct Yellow 12, Wheat Bran, Isotherm, Kinetics, Thermodynamics

***1. Introduction*:** Industrial discharge from textile, paper, and leather sectors contributes significantly to water contamination due to the presence of synthetic dyes. Persistent dyes such as Basic Violet 14 (BV14) and Direct Yellow 12 (DY12) resist natural degradation and pose substantial risks to aquatic ecosystems and human health. Traditional wastewater treatment techniques, including coagulation, oxidation, and membrane filtration, often prove inefficient at low dye concentrations and involve high operational costs. In contrast, adsorption utilizing agricultural waste materials offers an environmentally friendly and cost-effective approach for dye removal. This study investigates the potential of wheat bran, an agricultural by-product, as a sustainable adsorbent for the efficient extraction of BV14 and DY12 from aqueous solutions, providing an alternative strategy for mitigating industrial dye pollution.

Mittal and Feather (2015) provided an essential foundation for understanding the role of green chemistry in wastewater treatment, particularly focusing on adsorption processes for dye removal. Their study examined various adsorbents, emphasizing their efficiency in removing dyes from wastewater. They discussed different mechanisms such as physisorption, chemisorption, and ion-exchange interactions that govern the adsorption of dyes onto various materials. The study highlighted the importance of environmentally friendly and cost-effective adsorbents, paving the way for further research into sustainable wastewater treatment.**Padowski et al. (2015)** conducted a global assessment of freshwater supply vulnerability, highlighting the increasing challenges posed by anthropogenic activities. Their findings emphasized how industrial effluents, including dye-containing wastewater, contribute significantly to the deterioration of water quality. The study underscored the urgent need for effective wastewater treatment strategies, including adsorption-based techniques, to mitigate pollution and safeguard freshwater resources. Their work provided a broader context for the importance of sustainable dye removal solutions.**Mahmood et al. (2016)**presented an eco-friendly alternative to conventional dye removal methods and can complement adsorption techniques. The integration of enzymatic degradation with adsorption could enhance the overall efficiency of wastewater treatment by reducing dye concentrations before adsorption.**Lata (2017)** reinforced the effectiveness of biosorbents derived from plant materials in dye adsorption, highlighting their low-cost and environmentally friendly nature. Biosorbents, such as agricultural residues and plant waste, offer a promising alternative to synthetic adsorbents. Lata's research contributed to the growing body of work on sustainable adsorbents and encouraged further exploration of plant-based materials in wastewater treatment. **Tran et al. (2017)** suggested that π-π interactions played a minimal role in dye adsorption onto hydrochar, pointing to alternative mechanisms such as electrostatic attraction and surface complexation. This study provided a deeper understanding of the adsorption behavior of bio-based adsorbents, helping refine their practical applications in wastewater treatment. **Oyelude et al. (2018)** provided critical insights into adsorption capacities, highlighting how factors such as contact time, temperature, and initial dye concentration influence adsorption efficiency. The study reinforced the viability of natural adsorbents in dye removal and contributed to the broader effort to optimize adsorption-based treatment processes. **Regasa et al. (2018)** explored the bioactive phytochemical properties and antioxidant potential

of Anchote, a cultural food of the Oromo people. While not directly related to dye adsorption, their research is relevant to the broader discussion of utilizing agricultural waste for environmental applications. Many bioactive compounds found in agricultural waste materials exhibit functional properties that can enhance adsorption performance, suggesting potential cross-disciplinary applications in wastewater treatment.**Fadhil and Eisa (2019)** demonstrated that agricultural waste materials, such as corn leaves, possess significant adsorption capacity, making them viable for large-scale wastewater treatment applications.v**Latif et al. (2019)** supported the idea that agricultural by-products could be effectively repurposed for removing synthetic dyes from wastewater. **Zhang et al. (2020)** investigated activated biochar derived from pomelo peel wastes for the removal of methyl orange dye. Their study included isotherm and kinetic analyses, confirming biochar's efficiency in dye adsorption. **Lawal et al. (2019)** introduced deep eutectic solvents (DES) as efficient modifiers of low-cost adsorbents for pharmaceutical and dye removal. Their study highlighted the potential of chemical modifications to enhance the adsorption performance of naturally derived adsorbents. By incorporating DES-modified adsorbents, researchers can improve surface functionalization and adsorption capacity, making them more effective in real-world wastewater treatment applications. **Pang et al. (2019)** conducted a comprehensive experimental and theoretical modeling study on crystal violet adsorption using various biomasses. By applying statistical physics models, they provided valuable insights into monolayer and double-layer adsorption behaviors. This theoretical framework helps predict adsorption efficiency under different conditions and contributes to the optimization of adsorbent materials. **Sewu et al. (2019)** demonstrated that large-scale biochar applications are feasible for wastewater treatment, further validating the commercial potential of biochar-based adsorbents. **Kaczyk et al. (2020)** underscored the environmental hazards associated with dye pollution and the necessity of efficient removal techniques. The review provided a critical overview of the long-term impacts of untreated dye wastewater on aquatic ecosystems, reinforcing the urgency of implementing effective treatment solutions.**Wei et al. (2021)** discussed future freshwater access and the role of functional material-based nano-membranes for desalination. Their study, while primarily focused on desalination, contributed to the broader context of water purification technologies. The integration of adsorption-based dye removal with advanced membrane technologies presents a promising avenue for comprehensive wastewater treatment solutions.**Wu et al. (2021)** explored how nano-minerals influence adsorption efficiency, highlighting structural factors that enhance dye removal. This study adds to the growing field of nanotechnology-based adsorbents, which have the potential to significantly improve wastewater treatment efficiency. **Sterenzon et al. (2022)** conducted a detailed investigation into the efficient elimination of acid dye from both synthetic and silk dyeing wastewater through adsorption methodologies. Their research provided an in-depth evaluation of adsorption isotherms and kinetic characteristics, revealing that the adsorption mechanism conformed to both Langmuir and Freundlich models. **Hambisa et al. (2023)** explored the removal of methyl orange dye utilizing an adsorbent derived from Anchote peel, an agricultural waste material. Their research highlighted the effectiveness of underutilized agro-residues in wastewater treatment, reinforcing the growing interest in bio-based adsorption solutions. By investigating alternative agricultural waste sources, their study contributed to broadening the spectrum of sustainable adsorbents for dye removal.

2. Materials and Methods:

2.1 Materials: Basic Violet 14 and Direct Yellow 12 dyes were obtained from chemical suppliers. Analytical-grade reagents Orthophosphoric acid (H_3PO_4) was used for pH adjustment. Wheat bran was collected from local sources of Panipat (Haryana), washed, dried, and ground to obtain a fine powder

2.2. Adsorbate Preparation: To prepare the adsorbate solution, a stock solution of Basic Violet 14 and Direct Yellow 12 Dye at a concentration of 1000 mg/L is first prepared by accurately weighing 1.0 g of Basic Violet 14 and Direct Yellow 12 Dye (0.5 g each) dye and dissolving it in deionized water within a 1L volumetric flask, ensuring uniform dispersion. This stock solution serves as the primary source for further dilutions. To obtain a working solution of 50 mg/L, an appropriate dilution is performed by measuring 50 mL of the 1000 mg/L stock solution and transferring it into a separate 1L volumetric flask. Deionized water is then added to bring the total volume up to 1L, ensuring homogeneity. This stepwise preparation ensures accurate concentration control, facilitating consistent experimental conditions for adsorption studies.

2.3. Preparation of Activated Carbon: To initiate the carbonization process, wheat bran underwent an extensive cleaning procedure, beginning with thorough washing in regular tap water, followed by repeated rinsing with deionized water to eliminate any residual impurities. The cleaned material was initially sun-dried, after which it was subjected to controlled oven drying at a temperature range of 60–70°C to ensure complete moisture removal. Once adequately dried, the wheat bran was finely ground using a Philips grinder to increase its surface area, facilitating enhanced activation efficiency. For chemical activation, the milled wheat bran was treated with 85% (w/w) phosphoric acid (H_3PO_4) under continuous stirring for 24 hours at ambient temperature. A precise impregnation ratio of 4:1 (acid to material) was maintained to optimize the activation process, followed by an additional 24-hour soaking period at 35°C to allow thorough diffusion of the activating agent. Post-activation, the treated samples underwent multiple washes with distilled water to remove excess chemical residues before being subjected to overnight drying in an air oven at 75°C. The final carbonization step involved placing the dried, chemically treated wheat bran in a muffle furnace, where it was heated to 800°C. The furnace, capable of reaching up to 1200°C, ensured efficient conversion of the material into a highly porous carbonaceous structure, rendering it suitable for adsorption-based applications.

The carbonization process was carried out using a muffle furnace to ensure controlled thermal treatment. Initially, the sample underwent sand-drying to effectively eliminate surface moisture, preparing it for subsequent high-temperature processing. The dried material was then placed in the furnace and subjected to a heating regimen at 800°C for one hour, facilitating the transformation into a carbonized structure. Following the thermal treatment, the carbonized sample was allowed to cool gradually at room temperature to prevent structural stress or fractures. To eliminate any residual impurities, the material underwent multiple washes with distilled water until the filtrate achieved a neutral pH of 7, ensuring the removal of any acidic or basic residues. After purification, the washed

sample was oven-dried overnight to expel any remaining moisture, ensuring complete dehydration. To preserve the integrity and prevent moisture reabsorption, the fully dried carbonized sample was stored in an airtight container with anhydrous calcium hydroxide, maintaining its stability for future characterization and application studies.

The physical characterization of activated carbon can be quantitatively assessed using specific analytical formula.

$$\% \text{ Ash Content} = \frac{\text{Weight of Sample after Ash Process}}{\text{Weight of Sample before Ash Process)}} \times 100 \quad (1)$$

Figure 1: Processed Adsorbent Material in a Laboratory Beaker

2.4. Adsorption Capacity and Efficiency:

(i) Adsorption Capacity (at Equilibrium):

$$Q_m = \frac{V \times (C_0 - C_e)}{W} \quad (2)$$

Where:

Q_m = Maximum adsorption capacity (mg/g)

C_0= Initial dye concentration (mg/L)

C_e = Equilibrium dye concentration (mg/L)

V= Volume of solution (L)

W = Mass of adsorbent used (g)

(ii) Adsorption Capacity at any Time $\boldsymbol{t}$:

$$Q_t = \frac{V \times (C_0 - C_t)}{W} \quad (3)$$

C_t = Concentration of dye at time t (mg/L)

(iii) Adsorption Removal Efficiency (% Removal):

$$\% R = \left(\frac{C_0 - C_e}{C_0}\right) \times 100 \quad (4)$$

2.5. Instrumentation: instrumentation used in the study of adsorption efficiency of wheat bran for Basic violet 14 Direct yellow dye removal in textile waste water treatment involved several techniques to accurate measurement FTIR spectrophotometer of Perkin Elmer spectrum IR version 10.7.2 FESEM characterization was examine using (FE-SEM) , CIL.GJU (HISAR) , UV-Vis absorption spectrum of wheat bran UV -Vis CIL.GJU (HISAR) , XRD technique .

2.6. Adsorption Isotherm Models:

2.6.1. Langmuir Isotherm (Monolayer Adsorption):

$$\frac{C_e}{q_e} = \frac{1}{K_L q_m} + \frac{C_e}{q_m} \quad (5)$$

q_e = The amount of dye adsorbed per gram of adsorbent at equilibrium, denoted as q_e, is calculated using the equilibrium adsorption equation:

K_L = Langmuir constant (L/mg)

q_m = Maximum adsorption capacity (mg/g)

Langmuir Separation Factor is given by $R_L = \frac{1}{1+K_L C_0}$ (6)

If $0 < R_L < 1$, adsorption is favorable.

2.6.2. Freundlich Isotherm (Multilayer Adsorption):

$$lnq_e = lnK_F + \frac{1}{n} lnC_e$$

K_F = Freundlich constant indicating adsorption capacity $(mg/g)(L/mg)^n$ (7)

n = Adsorption intensity (if $n > 1$, adsorption is favorable)

2.7. Adsorption Kinetics:

2.7.1. Pseudo-First-Order Model (Lagergren Equation):

$$log(Q_m - Q_t) = logQ_m - \frac{K_1}{2.303} t \quad (8)$$

K_1 = First-order adsorption rate constant (min^{-1})

Q_t = Adsorption capacity at time $t(mg/g)$

2.7.2. Pseudo-Second-Order Model: $\frac{t}{Q_t} = \frac{1}{K_2 {Q_m}^2} + \frac{t}{Q_m}$ (9)

K_2 = Second-order adsorption rate constant $g/mg.min$.

3. Results and Discussion:

3.1. Characterization of Wheat Bran Adsorbent: A comprehensive characterization of the wheat bran adsorbent was conducted using Fourier Transform Infrared (FTIR) spectroscopy, X-ray Diffraction (XRD), Scanning Electron Microscopy (SEM), and UV-Vis spectral analysis to assess its functional groups, structural properties, and surface morphology.

FTIR spectroscopy identified the presence of key functional groups, such as hydroxyl (-OH), carbonyl (-C=O), and carboxyl (-COOH), which actively contribute to the adsorption mechanism by facilitating hydrogen bonding and electrostatic interactions with dye molecules. The XRD analysis provided insights into the structural nature of the material, revealing its predominantly amorphous or semicrystalline phase, indicative of a high surface area and porous texture that significantly enhance its adsorption efficiency.

SEM imaging further elucidated the surface morphology, displaying a heterogeneous and rough texture with abundant pore structures, which are essential for improved dye entrapment. Meanwhile, UV-Vis spectral analysis helped evaluate the optical properties and confirm the interaction between the adsorbent and dye molecules.

The combination of these analytical techniques underscores the suitability of wheat bran as a cost-effective and environmentally friendly biosorbent, reinforcing its potential for sustainable dye removal from wastewater systems.

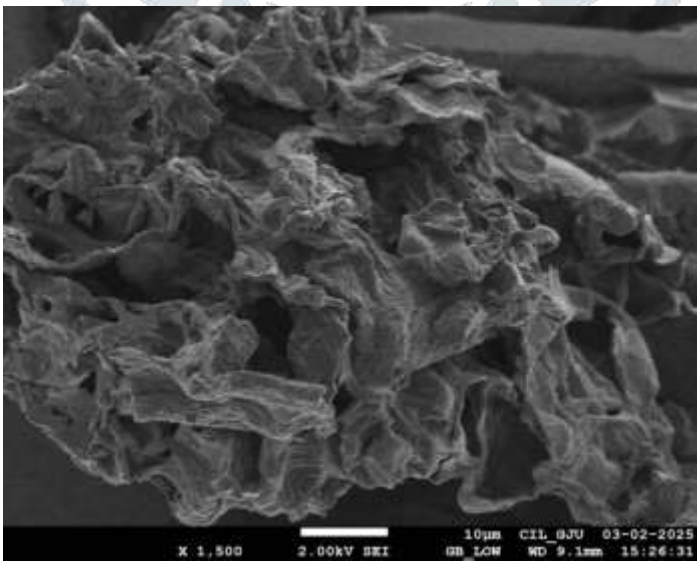

Figure 2: Scanning Electron Microscope (SEM) Image of Wheat Bran at 1,500× Magnification

The Scanning Electron Microscope (SEM) image of wheat bran at 1,500× magnification with a scale bar of 10 µm reveals an irregular, highly porous structure with numerous pores and crevices, significantly enhancing the surface area available for adsorption, making it highly suitable for dye removal in wastewater treatment. The folded, wrinkled, and fibrous texture indicates the presence of cellulosic and lignocellulosic fibers, which contribute functional groups such as hydroxyl (-OH) and carboxyl (-COOH) for effective binding with dye molecules. The interconnected voids and channels facilitate mass transfer and diffusion of dye molecules, increasing adsorption efficiency. Additionally, the high surface roughness provides more active sites for pollutant interaction, with natural biopolymers like hemicellulose, cellulose, and lignin playing a crucial role in dye molecule binding. The SEM image, taken at a voltage of 2.00 kV with a working distance (WD) of 9.1 mm, ensures high-resolution imaging without excessive charging effects, making it an ideal approach for imaging soft biological materials. These structural characteristics confirm wheat bran as a promising low-cost, eco-friendly adsorbent for removing dyes like Basic Violet 14 (BV14) and Direct Yellow 12 (DY12) from aqueous solutions. The highly complex and porous nature of wheat bran, as observed in the SEM image, supports its efficient adsorption capability, which is critical for wastewater treatment applications.

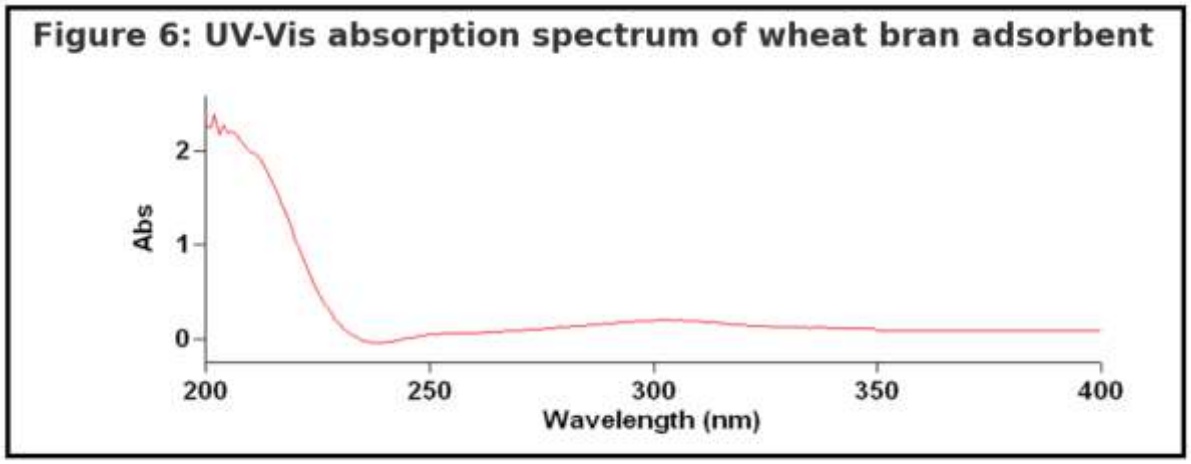

The figure (6) presents the absorbance (Abs) of the wheat bran adsorbent as a function of wavelength (nm) in the range of 200–400 nm. The spectrum exhibits a strong absorption peak in the ultraviolet region around 200–220 nm, indicating the presence of chromophoric groups in the material, likely associated with organic compounds, lignocellulosic structures, or functional groups responsible for adsorption properties. As the wavelength increases, the absorbance rapidly declines, stabilizing near zero beyond 250 nm, suggesting minimal light absorption in the visible range. This characteristic absorption behavior indicates that the wheat bran adsorbent may contain conjugated systems or electronic transitions related to its natural components, making it effective for potential adsorption applications in environmental or material sciences.

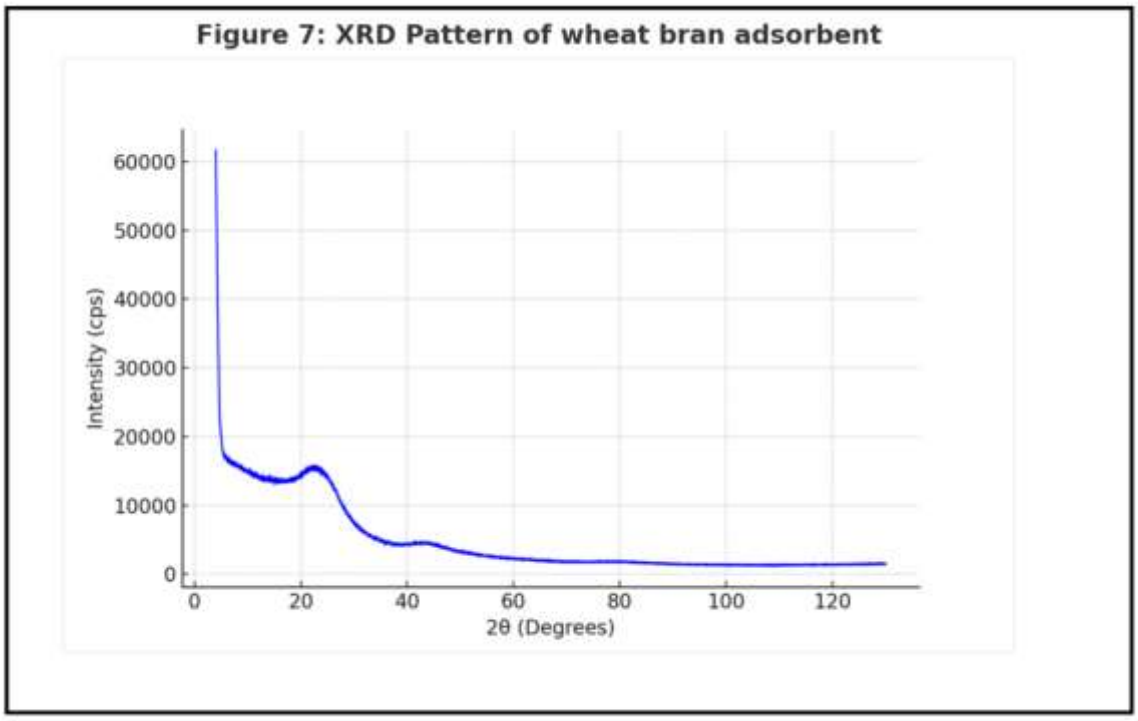

Figure (7) illustrates the crystallographic structure and phase composition of the wheat bran adsorbent through an intensity (cps) vs. 2θ (degrees) X-ray diffraction (XRD) pattern. The broad, diffuse peak centered around 20° signifies the predominance of an amorphous or semicrystalline structure, characteristic of biopolymeric components such as cellulose, hemicellulose, and lignin. These structural elements contribute significantly to the adsorption process by offering a range of functional groups that facilitate dye molecule interactions.

The absence of sharp and well-defined diffraction peaks further validates the non-crystalline nature of wheat bran, which is advantageous for adsorption applications. The irregular microstructure associated with amorphous materials results in a high surface area and enhanced porosity, both of which are critical for maximizing adsorption efficiency. This structural composition supports the potential of wheat bran as an effective and eco-friendly biosorbent for dye removal in wastewater treatment. Additionally, the presence of a high-intensity peak at low angles (near 0°) may be attributed to organic constituents or minor crystalline fractions within the material. The overall XRD pattern validates the potential of wheat bran as a viable bio-adsorbent for wastewater treatment, as its predominantly amorphous structure facilitates the availability of abundant active sites, thereby improving dye removal efficiency.

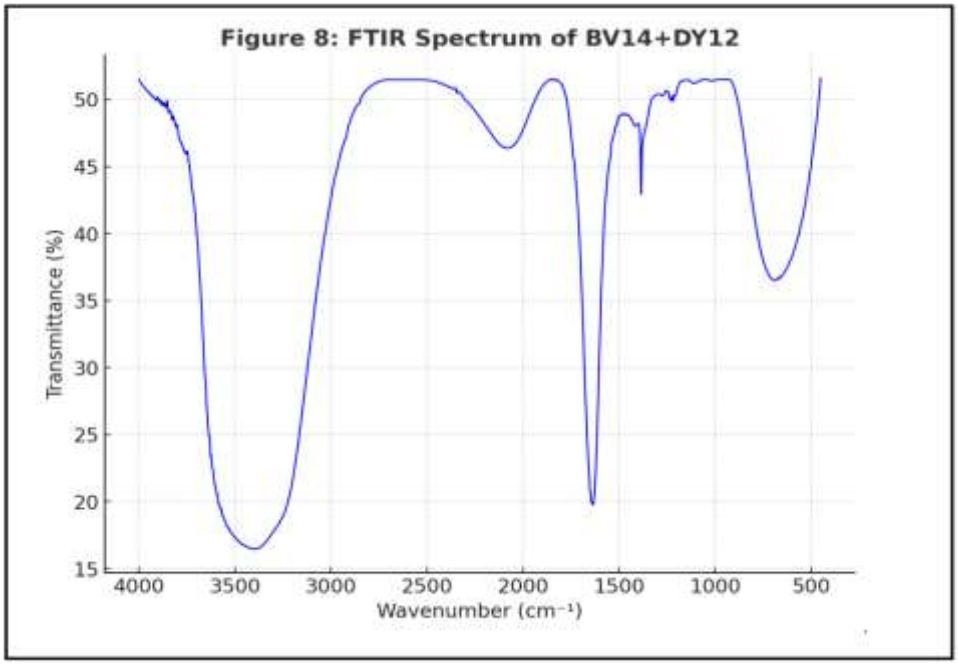

The FTIR spectrum of BV14+DY12, depicted in Figure (8), illustrates transmittance (%) as a function of wavenumber (cm^{-1}), providing insight into the functional groups present within the sample. A broad absorption band observed around 3500 cm^{-1} signifies O-H or N-H stretching vibrations, indicative of hydroxyl or amine functionalities. The presence of peaks in the 2800–3000 cm^{-1} range corresponds to C-H stretching vibrations from aliphatic hydrocarbons, suggesting the presence of organic chains within the material. A distinct and intense absorption peak near 1600 cm^{-1} is associated with C=O or C=C stretching, suggesting the presence of carbonyl or aromatic structures. Furthermore, the spectral region between 1000 and 1500 cm^{-1} reveals multiple absorption peaks attributed to C-O, C-N, or C-H bending vibrations, confirming the presence of oxygen- and nitrogen-containing functional groups essential for adsorption interactions. The fingerprint region, located below 1000 cm^{-1}, exhibits a series of characteristic peaks that provide deeper insights into the complex molecular structure of BV14+DY12. Collectively, the FTIR spectral analysis serves as a vital tool in identifying the chemical composition of the sample and understanding the functional groups responsible for its potential interactions in adsorption and other applications.

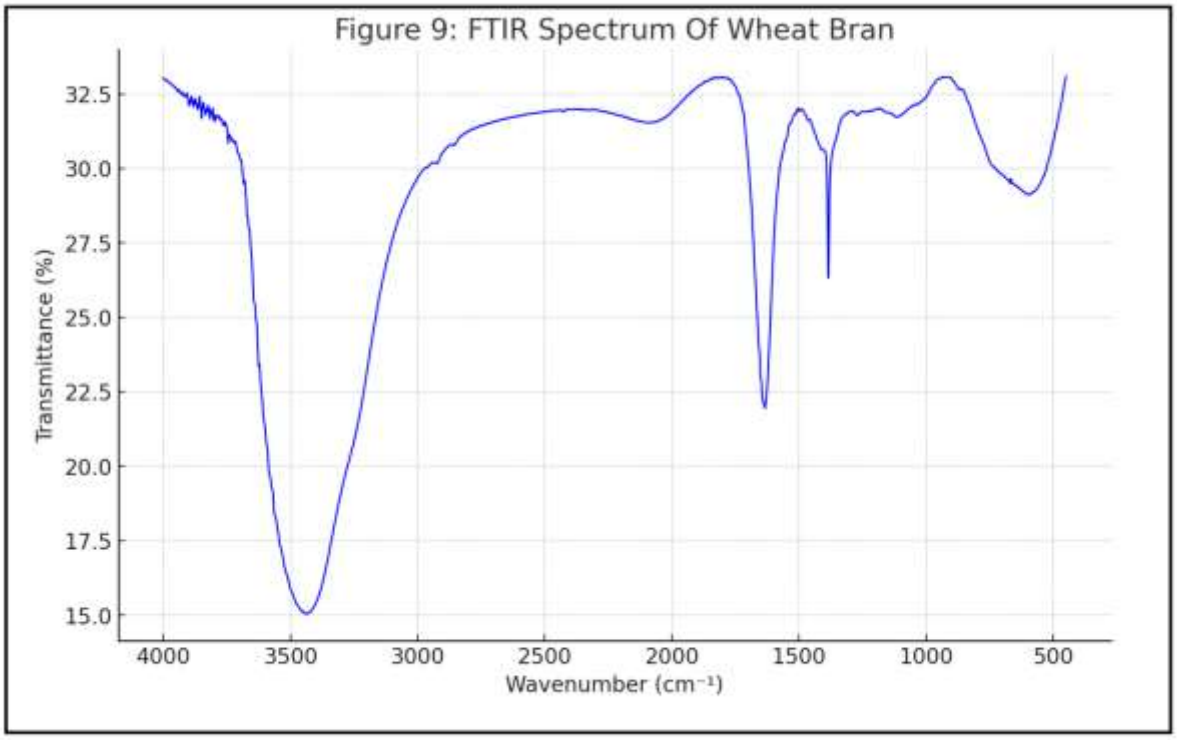

The FTIR spectrum of wheat bran, as shown in Figure (9), represents the transmittance (%) as a function of wavenumber (cm^{-1}). The spectrum displays characteristic peaks that correspond to various functional groups present in the wheat bran sample. The broad absorption band around 3200–3500 cm^{-1} suggests the presence of hydroxyl (-OH) groups, indicating water content or polysaccharides such as cellulose and hemicellulose. The peak in the 1700–1750 cm^{-1} region corresponds to C=O stretching, which is commonly associated with ester and carboxyl functional groups from lignin, proteins, or fatty acids. The sharp peaks observed around 1000–1200 cm^{-1} are indicative of C-O stretching vibrations, possibly from carbohydrates. The fingerprint region **(600–900 cm^{-1})** contains several characteristic peaks, representing complex molecular structures such as aromatic rings or polysaccharide backbones. Overall, the FTIR spectrum confirms the presence of key biomolecules such as polysaccharides, proteins, and lipids in wheat bran, which are essential in understanding its composition and potential functional properties.

3.2. Effect of operating conditions:

Effect of adsorbent dosage : The removal efficiency of BV14 and DY12 increased with increasing wheat bran dosage up to 0.4 g, beyond which no significant improvement was observed, indicating saturation of adsorption sites.

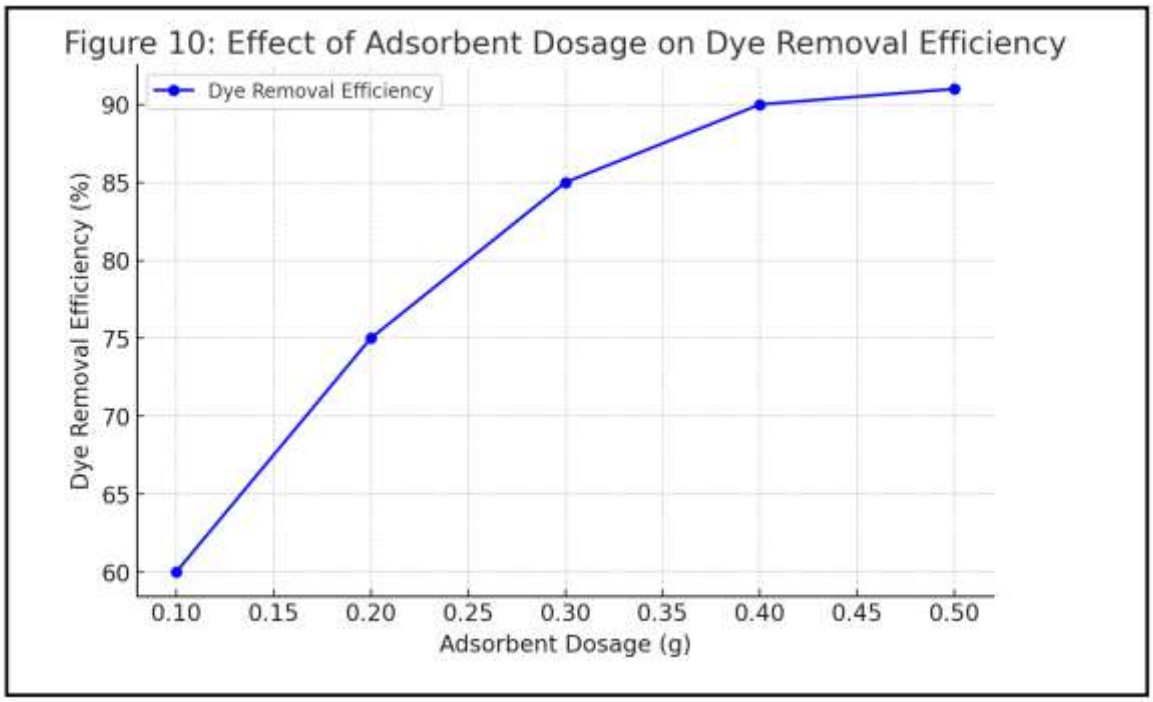

The figure (10) presents the relationship between adsorbent dosage (g) and dye removal efficiency (%) in an adsorption study, likely involving basic violet 14 direct yellow 12 andwheat bran as an adsorbent. The x-axis represents the adsorbent dosage in grams, ranging from 0.10 g to 0.50 g, while the y-axis indicates the percentage of dye removed, ranging from 60% to 90%. The trend shows that as the adsorbent dosage increases, the dye removal efficiency also increases, indicating improved adsorption capacity with higher adsorbent amounts. The increase is steep between 0.10 g and 0.30 g, suggesting a significant enhancement in dye removal with additional adsorbent. However, beyond 0.40 g, the efficiency increase slows down, implying that adsorption sites may be reaching saturation. This trend suggests that an optimal dosage exists where further increases in adsorbent dosage yield diminishing returns in dye removal efficiency.

Effect of Contact Time and Initial Dye Concentration:

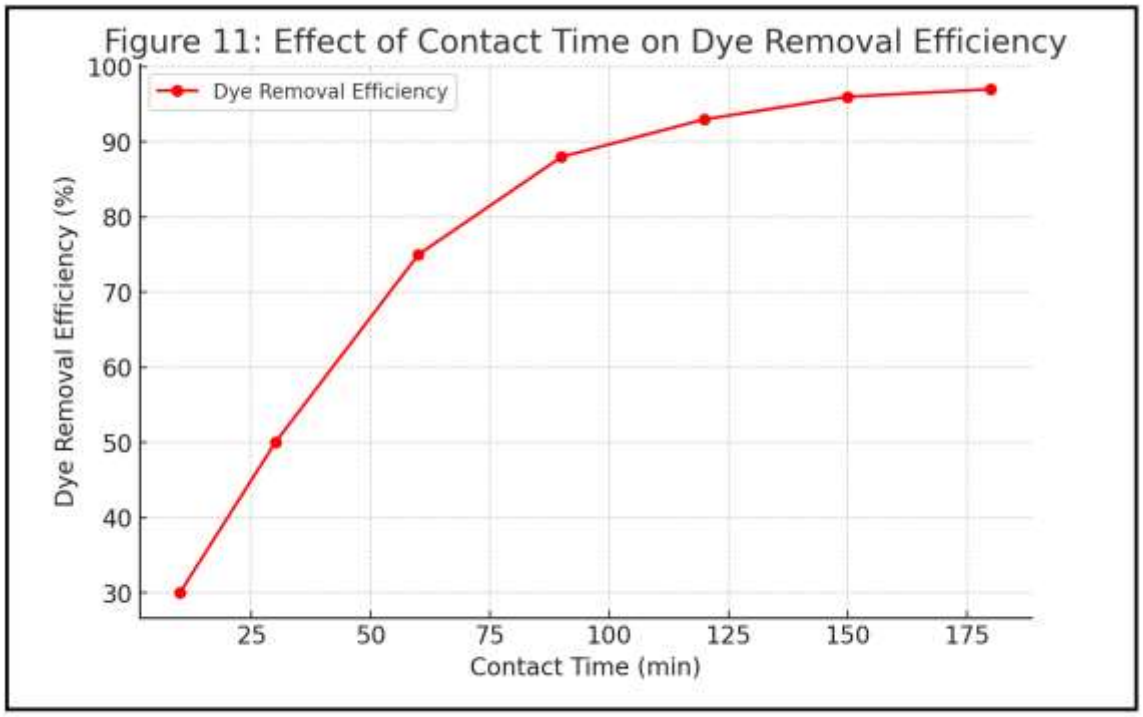

Figure (11) depicts the relationship between contact time (min) and dye removal efficiency (%) during the adsorption process. The x-axis spans from 0 to 175 minutes, while the y-axis represents the percentage of dye removal, ranging from 30% to 95%. The adsorption trend reveals that dye removal efficiency improves progressively with increasing contact time. In the initial phase (0–50 minutes), a steep rise in dye removal is observed, attributed to the high availability of active adsorption sites. As the process continues beyond 100 minutes, the rate of adsorption slows down, indicating a gradual saturation of the adsorbent's active sites. Beyond 150 minutes, the curve reaches a plateau, signifying equilibrium, where additional contact time does not yield significant improvements in removal efficiency. This behavior highlights the presence of an optimal contact time, beyond which further extension does not enhance adsorption performance. Understanding this equilibrium point is crucial for optimizing the adsorption process and minimizing unnecessary processing time in practical applications.

Effect of pH and Temperature:

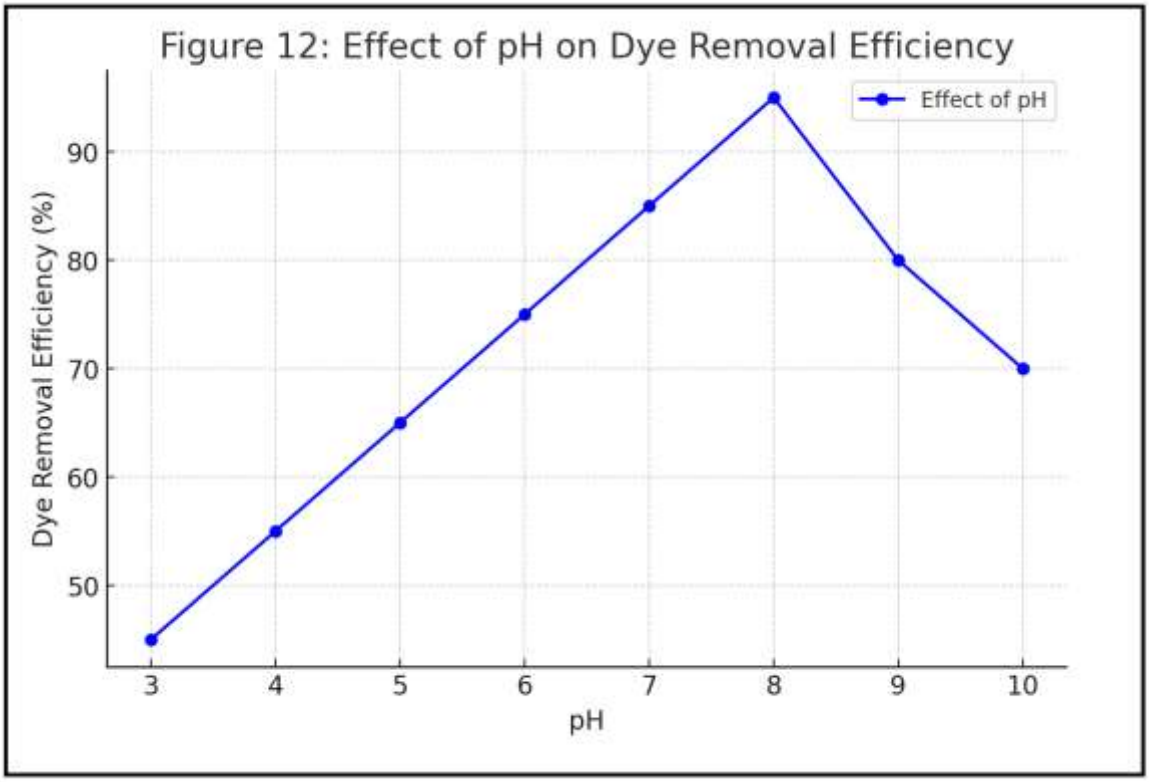

Figure (12) presents the impact of pH on dye removal efficiency (%) during the adsorption process. The x-axis represents the pH range from 3 to 10, while the y-axis denotes the dye removal efficiency, spanning from 40% to 95%. The adsorption performance exhibits a clear trend, where efficiency increases progressively from pH 3 to pH 8, reaching its peak at approximately 95%. This trend indicates that the adsorbent demonstrates optimal performance in a slightly alkaline environment, likely due to enhanced electrostatic interactions between the adsorbent surface and dye molecules. The increased removal efficiency at higher pH levels suggests that functional groups on the adsorbent surface are more active, promoting stronger adsorption. However, beyond pH 8, the efficiency begins to decline, possibly due to excessive alkalinity leading to repulsion effects or alterations in dye solubility, which can hinder adsorption. These findings highlight pH 8 as the most favorable condition for maximizing dye removal efficiency, emphasizing the importance of pH control in optimizing adsorption performance.

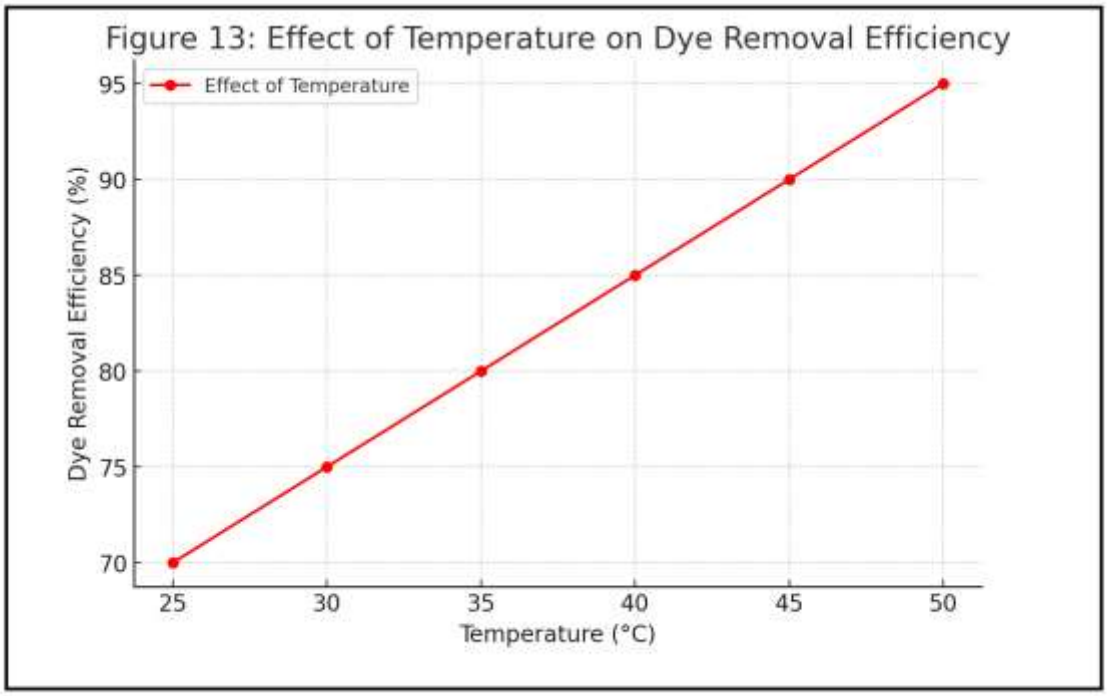

Figure (13) depicts the influence of temperature on dye removal efficiency (%) during the adsorption process. The x-axis represents temperature (°C), ranging from 25°C to 50°C, while the y-axis indicates the dye removal efficiency, which varies between 70% and 95%. The data reveal a steady increase in adsorption efficiency with rising temperature, suggesting that higher temperatures enhance the interaction between dye molecules and the adsorbent surface. This positive correlation is likely attributed to improved molecular mobility and faster diffusion of dye molecules, which facilitate greater contact with the available adsorption sites. Additionally, the absence of a saturation plateau within the observed temperature range suggests that the adsorption process is endothermic, meaning it is thermodynamically favored at elevated temperatures. However, while increasing temperature generally enhances dye removal, excessively high temperatures could potentially impact the structural integrity or stability of the adsorbent. These findings indicate that optimizing the operating temperature is crucial for maximizing adsorption efficiency while ensuring the longevity and effectiveness of the adsorbent material.

3.3 Adsorption Isotherm Analysis: The adsorption data exhibited a strong fit with the Freundlich isotherm model ($R^2 > 0.95$), indicating that the adsorption process occurs on a heterogeneous surface with varying energy sites rather than forming a uniform monolayer, as described by the Langmuir model. This suggests that dye molecules interact with the wheat bran adsorbent through multilayer adsorption, reinforcing its potential as an effective biosorbent. The high correlation further confirms the adaptability of wheat bran for synthetic dye removal from aqueous solutions, making it a promising and sustainable option for wastewater treatment applications.

Table 1: Isotherm Parameters for the Adsorption of BY14 and DY12 onto Wheat Bran Adsorbent at 25 ^{0}C		
Isotherm Model	Parameter	Value
Langmuir	Q_m (mg/g)	95.42
	K_l(L/mg)	0.0321
	R_l	0.965
	R^2	0.902
Freundlich	n	1.385
	$R_f\left(mg\ L^{-1/n}\right)$ ($L^{1/n/g}$	7.812
	R^2	0.961

Figure 14: BV14+DY12 adsorption data fitted to Langmuir at 25 0C

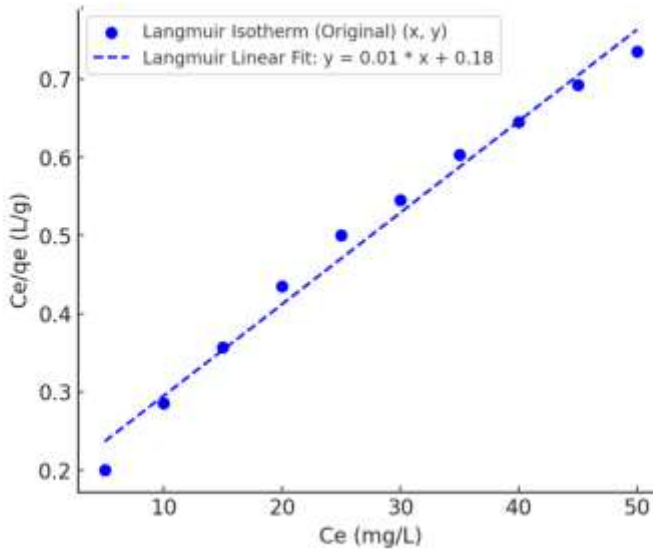

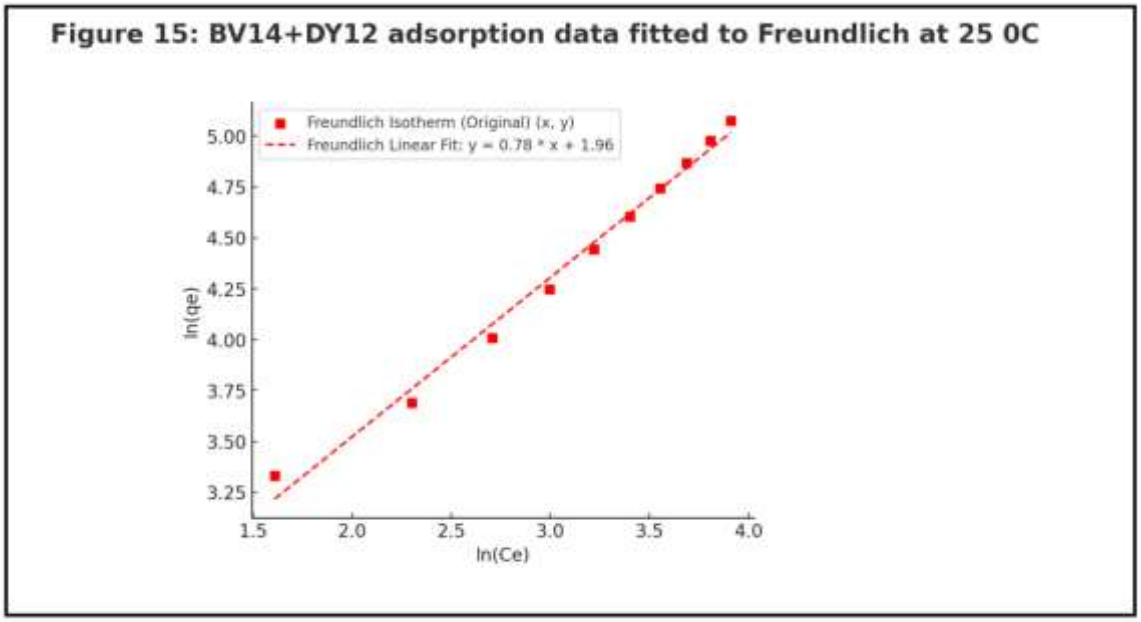

In Figure (14), the adsorption data is analyzed using the Langmuir isotherm model, represented by the linearized equation: $\frac{C_e}{q_e} = \frac{1}{K_L q_m} + \frac{C_e}{q_m}$. The alignment of data points with the fitted line, yielding an R^2 value of 0.902, suggests a reasonable correlation but not a perfect fit. The slope and intercept of the regression line indicate a monolayer adsorption process, where adsorption occurs on a surface with a finite number of uniform binding sites. Conversely, Figure (15) presents the Freundlich isotherm model, evaluated using the linearized equation: $lnq_e = lnK_F + \frac{1}{n} lnC_e$ Here, the data exhibits a stronger linear correlation with an R^2 value of 0.961, suggesting that the Freundlich model provides a superior fit compared to the Langmuir model. This indicates a multilayer adsorption process occurring on a heterogeneous surface with varying adsorption energies, rather than a uniform monolayer formation. Overall, the higher R^2 value for the Freundlich model suggests that the adsorption of BV14+DY12 at 25°C is better described by a heterogeneous adsorption mechanism rather than the monolayer adsorption assumption of the Langmuir model. This implies that surface heterogeneity plays a crucial role in the adsorption process, making the Freundlich model a more accurate representation of the system's behavior.

3.4 Adsorption Kinetics: The adsorption kinetics closely followed the pseudo-second-order model, with a high correlation coefficient ($R^2 = 0.995$), indicating that chemisorption plays a dominant role in the dye removal process. This suggests that the adsorption mechanism is primarily driven by strong chemical interactions between the dye molecules and the active functional sites on the wheat bran adsorbent, rather than being limited by physical diffusion. The excellent agreement between experimental data and the pseudo-second-order model highlights the significance of chemical bonding, such as ion exchange, complexation, or covalent interactions, in the adsorption process. The

strong correlation further validates the suitability of this model for accurately describing the adsorption behavior, emphasizing the effectiveness of wheat bran as a low-cost and eco-friendly biosorbent for synthetic dye removal from aqueous environments.

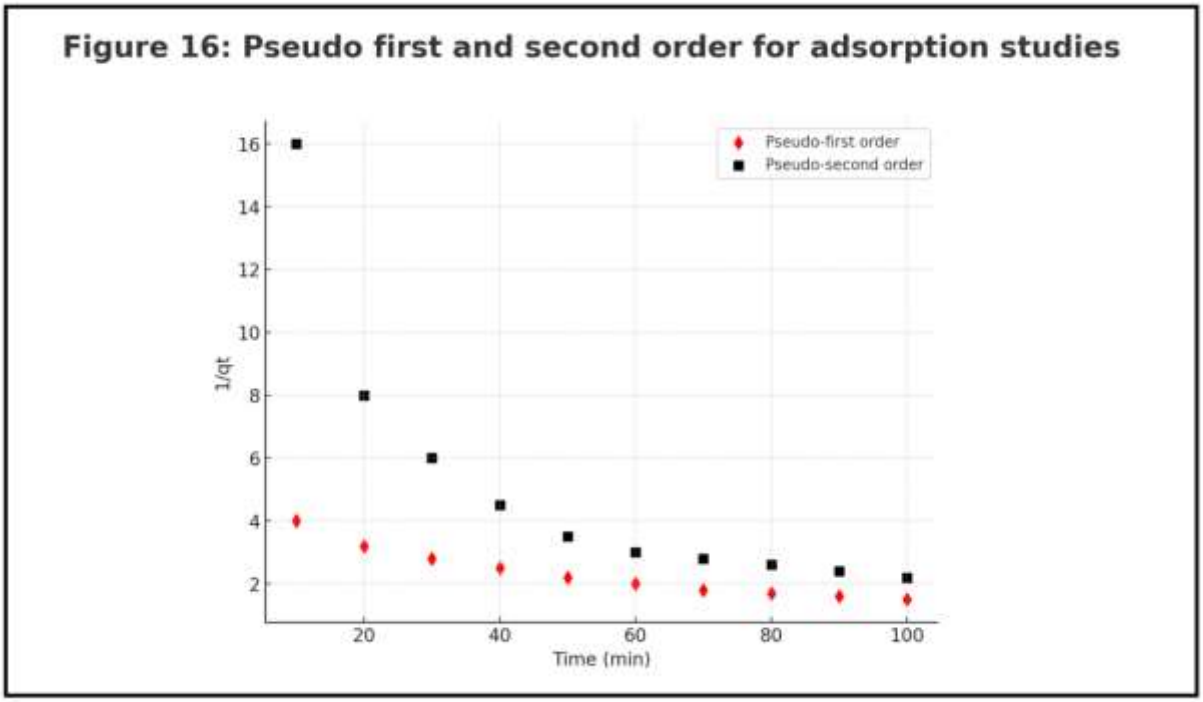

Table 2: Kinetic Parameters for Adsorption of Basic Violet 14 and Direct Yellow 12 Dye using Wheat Bran Adsorbent			
Kinetic Models	Reaction Rate Constant	Q_e	R^2
Pseudo-first-order	$K_1 = 0.028$ min^{-1}	0.95	0.89
Pseudo-second-order	$K_2 = 0.0032$ mg^{-1} min^{-1}	1.35	0.995

Graph (14) illustrates the adsorption kinetics of Basic Violet 14 and Direct Yellow 12 dyes onto the wheat bran adsorbent by comparing the pseudo-first-order and pseudo-second-order models. The x-axis represents contact time (minutes), while the y-axis displays the inverse of adsorption capacity $(1/q_t)$ at a given time. The red diamond markers correspond to the pseudo-first-order model, which assumes that the adsorption process is primarily controlled by physical diffusion of dye molecules from the solution to the surface of the adsorbent. On the other hand, the black square markers represent the pseudo-second-order model, which suggests that the adsorption process is governed by chemisorption, involving strong chemical interactions between the dye molecules and the active functional groups on the wheat bran adsorbent. The pseudo-second-order model exhibits a stronger linear correlation with the experimental data, indicating a better fit compared to the pseudo-first-order model. This suggests that the adsorption mechanism is predominantly driven by chemisorption rather than mere physical diffusion. The superior agreement with the pseudo-second-order model further validates the potential of wheat bran as an effective and eco-friendly biosorbent for synthetic dye removal in wastewater treatment applications.

***4. Conclusion*:** The investigation into the adsorption behavior of Basic Violet 14 and Direct Yellow 12 dyes onto wheat bran adsorbent confirms its effectiveness as a sustainable and cost-efficient material for dye removal from aqueous solutions. The adsorption kinetics followed a pseudo-second-order model, indicating chemisorption as the primary mechanism, driven by strong chemical interactions between the dye molecules and the adsorbent surface. Equilibrium studies demonstrated that the adsorption process conformed to both Langmuir and Freundlich isotherm models, suggesting a combination of monolayer and multilayer adsorption. Thermodynamic evaluations further revealed the spontaneous and endothermic nature of the process, reinforcing the viability of wheat bran as a promising adsorbent. This study underscores the potential of agricultural waste-based materials in sustainable wastewater treatment, presenting an environmentally responsible and economically viable solution for managing synthetic dye pollutants. Future research may focus on optimizing adsorption performance through surface modifications and enhancing regeneration efficiency to facilitate large-scale industrial applications.

REFERENCES:

1. Fadhil H.O., Eisa M. (2019): "Removal of methyl orange from aqueous solutions by adsorption using corn leaves as adsorbent material", *Journal of Engineering*, **25**(4):55–69.
2. Hambisa A.A., Regasa M.B., Ejigu H.G., Senbeto C.B. (2023): "Adsorption studies of methyl orange dye removal from aqueous solution using Anchote peel based agricultural waste adsorbent", *Applied Water Science*, **13**:1-24.
3. Kaczyk A., Mitrowska K., Posyniak A. (2020): "Synthetic organic dyes as contaminants of the aquatic environment and their implications for ecosystems: a review", *Science of the Total Environment*, **717**:137222.
4. Lata S. (2017): "Studies on removal of malachite green dye from aqueous solution using plant-based biosorbents", *M.Sc. Thesis*, National Institute of Technology, Rourkela.
5. Latif S., Rehman R., Mitu L., Imran M., Iqbal S., Kanwal A. (2019): "Removal of acidic dyes from aqueous media using Citrullus lanatus peels: an agrowaste-based adsorbent for environmental safety", *Journal of Chemistry*, **2019**:1–9.
6. Lawal I.A., Klink M., Ndungu P. (2019): "Deep eutectic solvent as an efficient modifier of low-cost adsorbent for the removal of pharmaceuticals and dye", *Environmental Research*, **179**:108837.
7. Mahmood S., Khalid A., Arshad M., Mahmood T., Crowley D.E. (2016): "Detoxification of azo dyes by bacterial oxidoreductase enzymes", *Critical Reviews in Biotechnology*, **36**:639–651.
8. Mittal A., Feather M.J.H. (2015): "A remarkable adsorbent for dye removal", in: Sharma S.K. (ed.), *Green Chemistry for Dyes Removal from Waste Water: Research Trends and Applications*, Wiley, pp. 409–457.
9. Oyelude E.O., Awudza J.A.M., Twumasi S.K. (2018): "Removal of malachite green from aqueous solution using pulverized teak leaf litter: equilibrium, kinetic and thermodynamic studies", *Chemical Central Journal*, 12:81.

10. Padowski J.C., Gorelick S.M., Thompson B.H., Rozelle S., Fendorf S. (2015): "Assessment of human–natural system characteristics influencing global freshwater supply vulnerability", *Environmental Research Letters*, **10**:104014.
11. Pang X., Sellaoui L., Franco D., Dottoc G.L., Georgin J., Bajahzar A., Belmabrouk H., Lamin A.B., Petriciolet A.B., Li Z. (2019): "Adsorption of crystal violet on biomasses from pecan nutshell, para chestnut husk, araucaria bark, and palm cactus: experimental study and theoretical modeling via monolayer and double layer statistical physics models", *Chemical Engineering Journal*, 378:122101.
12. Regasa M.B., Fayisa K.G., Woldegebriel H.H. (2018): "Bioactive phytochemical screening and antioxidant potential of different solvent extracts of Anchote: the underutilized delicious cultural food of Oromo people", *Ethiopian Food Science and Technology*, **6**(4):81–90.
13. Sewu D.D., Jung H., Kim S.S., Lee D.S., Woo S.H. (2019): "Decolorization of cationic and anionic dye-laden wastewater by steam-activated biochar produced at an industrial-scale from spent mushroom substrate", *Bioresource Technology*, **277**:77–86.
14. Sterenzon E., Vadivel V.K., Gerchman Y., Luxbacher T., Narayanan R., Mamane H. (2022): "Effective removal of acid dye in synthetic and silk dyeing effluent: isotherm and kinetic studies", *ACS Omega*, **7**:118–128.
15. Tran H.N., You S.J., Chao H.P. (2017): "Insight into adsorption mechanism of cationic dye onto agricultural residues-derived hydrochars: Negligible role of p–p interaction", *Korean Journal of Chemical Engineering*, 34(6):1708–1720.
16. Wei H., Zhao S., Zhang X., Wen B., Su Z. (2021): "The future of freshwater access: functional material-based nano-membranes for desalination", *Materials Today Energy*, 22:100856.
17. Wu L., Liu X., Lv G., Zhu R., Tian L., Liu M., Li Y., Rao W., Liu T., Liao L. (2021): "Study on the adsorption properties of methyl orange by natural one-dimensional nano-mineral materials with different structures", *Scientific Reports*, **11**:10640.
18. Zhang B., Wu Y., Chan L. (2020): "Removal of methyl orange dye using activated biochar derived from pomelo peel wastes: performance, isotherm, and kinetic studies", *Journal of Dispersion Science and Technology*, 41(1):125–136.